JOURNAL OF MATERIALS SCIENCE 35 (2000) 3131–3141

Sintering properties of submicron TiC powders from carbon coated titania precursor

R. KOC*, CHANG MENG‡, G. A. SWIFT§
Department of Mechanical Engineering and Energy Processes, Southern Illinois University at Carbondale, Carbondale, IL 62901, USA
E-mail: rkoc@mse.ufl.edu

The sintering behavior of submicron titanium carbide (TiC) synthesized from carbon coated titania (TiO_2) precursor was investigated in TiC-Ni system. The densification was examined as functions of initial carbon content (30.95–34 wt.%) and Ni content (3–20 wt.%). The sintered density of TiC-Ni was markedly decreased with increased carbon content in the precursor. The amount of Ni had a relatively small influence on the densification of submicron TiC-Ni cermet compared with TiC (commercially available HCS)-Ni cermets. The results show that submicron TiC with only 3 wt.% Ni can be sintered to densities above 95% TD in flowing $Ar+10H_2$ at 1500°C and below. The improvements in densification result from the capillary force increase since it is inversely dependent on the particle size. With decreased Ni content, the Vickers hardness increased and the fracture toughness decreased, as expected. However, the sufficient densification cannot be achieved for commercial HCS TiC powder sintered with Ni (<10 wt.%) under the same conditions. Therefore, both the Vickers hardness and fracture toughness decreased as the Ni content decreased. This was due to the increase of porosity in the sintered samples containing commercial TiC powder.

1. Introduction

Carbides belong to a broad class of compounds having a number of valuable properties. Metal carbides, particularly carbides of the transition metals, are applied in industries from refractories to cutting tools, from electronics to chemical resistant structural applications. Titanium carbide is a prominent material in these types of applications. It combines the advantages of a high melting point (3260°C), high hardness (Knoop's = 32.4 GPa), high electrical conductivity (30×10^6 1/ohm·cm), high chemical and thermal stability, high wear resistance, high solvency for other carbides, and a low density (4.93 g/cm^3).

Titanium carbide is often combined with metals, such as nickel, to form cermets, or cemented carbides, which have properties superior to those of either constituent. Cermets they combine very high hardness and wear resistance of their carbide phase with the mechanical and thermal shock resistance provided of the metallic binder phase. These properties make them useful for many applications involving large mechanical and thermal stresses. Titanium carbide based cermets are often used in the manufacture of cutting tools, grinding wheels, and coated cutting tips [1].

The properties of TiC-Ni cermets depend on the microstructure. The ideal microstructure desired for TiC-Ni cermets can only be achieved through use of high quality TiC powder with controlled levels of purity and morphology. The carbon coating method utilized in this research is patented and it is the only method in the literature which produces submicron size TiC powder at low cost [2]. Detailed information on the effect of amount of carbon in the precursor on the characteristics of resulting TiC powder will be addressed in a separate paper. The present work attempts to provide information on the sintering behavior of submicron TiC powder with various sintering parameters.

TiC based cermets are typical examples of systems undergoing liquid phase sintering resulting in a two-phase material with ductile behavior despite a large quantity of hard phase. The classic treatment of persistent liquid phase sintering breaks the process into three stages [3]: 1) rearrangement, 2) solution-reprecipitation, 3) and coalescence. Capillary forces are enhanced by smaller particles, increasing the rate of rearrangement in stage (1). This occurs despite higher levels of friction between particles. Similarly, the rate of densification in stage (2) is improved using fine powders. Previous research involving persistent liquids indicates superior densification and improved mechanical properties result from use of smaller particles [4].

In the present study, first, submicron TiC powders with different carbon contents using carbon coating precursor method were produced and characterized. In this

* *Present Address*: Department of Materials Science and Engineering, University of Florida, Gainesville, FL 32611.
‡ *Present Address*: Adecco TAD Technical, Peoria, IL 61615.
§ *Present Address*: Department of Materials Science, California Institute of Technology, Pasadena, CA 91125.

step, emphasis was placed in noting the effect of variable initial carbon content on the resulting TiC powder. In the second step, the sintering of the as-produced submicron TiC powder was examined with emphasis placed on the effect of carbon and nickel contents on the densification.

2. Experimental procedure

TiC powders were produced using the carbon coating process that was first described by Koc *et al*. [5]. The process consists of two steps. The first step is the coating of TiO_2 (P25 Degussa Corp., Ridgefield Park, NJ) with carbon by decomposing a hydrocarbon gas (C3H6) at temperature of 550°C. This step was performed in a rotating chamber furnace consisting of a 10 cm ID×35 cm stainless steel cylinder. About 200 grams of TiO_2 powder was placed in the vessel. The vessel was evacuated, purged with argon, and evacuated again. The vessel was then heated to 550°C and filled with propylene gas until the pressure reached about 3 atm. After approximately 5 minutes the remaining gas was released and the vessel was filled with fresh propylene. The coating step was continued until the desired amount of carbon was deposited. Three precursors were prepared containing 30.95 wt.% (30F), 32 wt.% (32F), and 34 wt.% (34F) carbon. The weight percentage of the carbon in the precursors was determined using thermogravimetric analysis in air. The second step involves the formation of TiC powders by promoting the carbothermal reduction of the carbon coated TiO_2 precursors at 1550°C for four hours in a flowing argon gas (1L/min). This step was performed in an atmosphere-controlled tube furnace (Model CTF 17/75/300, Carbolite, Sheffield, UK) with 70 mm ID.

The precursor material and produced TiC powders were characterized using X-ray diffraction (XRD) (Rigaku,Tokyo, Japan) with Cu K_α radiation, a BET surface area analyzer (Micromeritics, Gemini 2360, Norcross, GA), and transmission electron microscopy (TEM) (Hitachi, Model FA 7100, Tokyo, Japan). Oxygen and total carbon contents of the TiC powders were determined by the LECO corporation (St. Joseph, OH). XRD was utilized to determine the phase constitution of the powders, and, using Ni as an internal standard, the lattice parameter of produced TiC was determined. The samples with 35 wt.% Ni was scanned from 25° to 140° (2θ value) with a step size of 0.02° and duration time of 1 s at each step. Lattice parameter values were obtained at each crystal plane and a was plotted as a function of $\cos^2\theta$. The least-squares line of the data was

$$a = a_0 + K' \cos^2 \theta \qquad (1)$$

where a_0 is the extrapolated value of a when $\cos^2\theta$ approaches 0 and K' is the slope of the least-squares line. TEM was used to investigate the particle size, size distribution, particle morphology and degree of agglomeration as a function of total carbon.

The produced TiC and Ni powders were mixed in a WC container together with two WC balls and alcohol using a Spex Model 8000 Mixer/Mill (Spex Corp., Metuchen, NJ). After 2 hours of mixing, the powder slurry was dried in a vacuum oven at 65°C. Pellets were made by single action, uni-axial pressing in a hardened steel die (ID = 12.95 mm). These pellets were made at different pressures to obtain green densities between 45% and 65% TD. Densification was conducted at 1500°C for 2 hours in flowing Ar-10%H_2 atmospheres in a tube furnace. Bulk densities of sintered pellets were determined by the liquid (xylene) displacement technique. Scanning electron micrographs of the polished surfaces of sintered specimens were taken in a model Hitachi S570 scanning electron microscope (SEM). Vickers hardness values were measured with LECO hardness tester using a load of 5 kg. The fracture toughness was determined using Vickers hardness indention method.

3. Results and discussion

Figs 1 and 2 show a TEM micrograph and the XRD pattern of the carbon- coated TiO_2 precursor, respectively. As shown in the figures, a very uniform coating of pyrolytic carbon on TiO_2 is apparent. All peaks correspond to starting TiO_2 (anatase and rutile) phase, implying that a pyrolytic amorphous form of carbon is deposited. The BET surface area of the coated TiO_2 precursors was measured to be in the range of 44–46 m^2/g after being coated with 30.95 wt.%, 32 wt.% and 34 wt.% carbon. These results showed that uniform carbon coating can be deposited at 550°C on TiO_2 particles by using C_3H_6 hydrocarbon gas. This way of introducing carbon forms an intimate mixing of the reactants (C and TiO_2) with high surface contact between carbon and titania. These precursors are capable of producing high-purity TiC powders at low temperatures, because

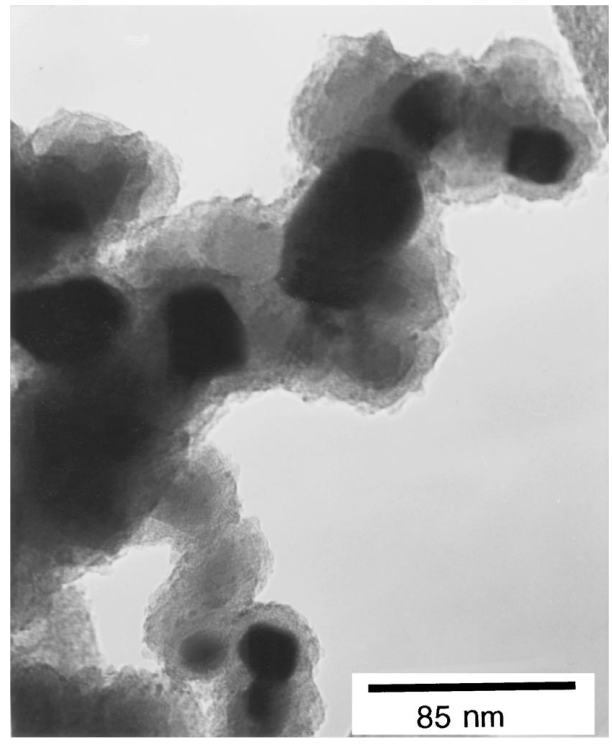

Figure 1 TEM micrograph of TiO_2 coated with 32 wt.% C.

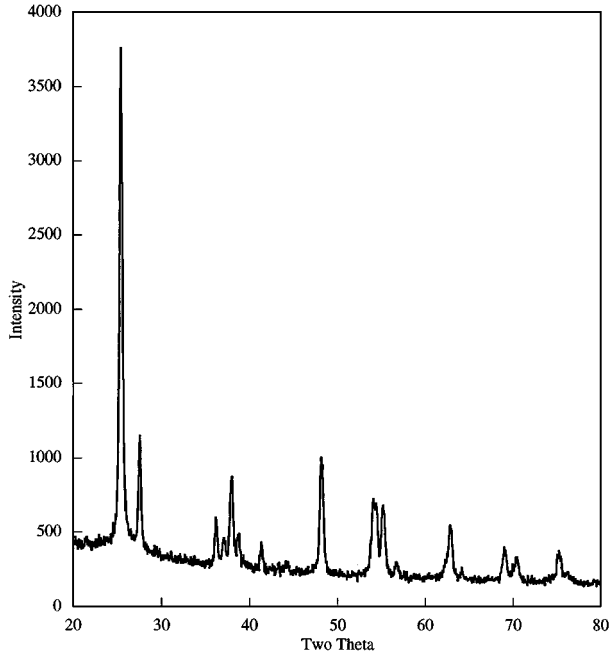

Figure 2 XRD result of TiO_2 coated with 32 wt.% C.

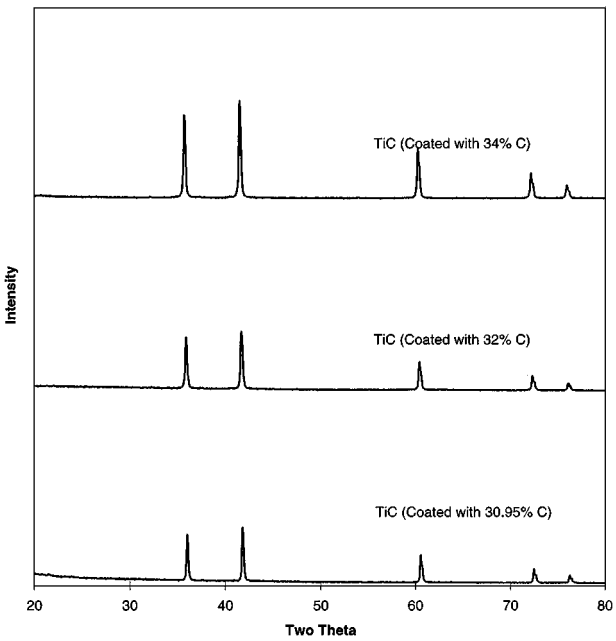

Figure 3 XRD results of reaction products from carbon coated TiO_2 reacted at 1550°C for 2 hours in flowing Argon (1L/M).

the carbon source for the reduction is from hydrocarbon gas. Therefore, impurities such as iron (which is ordinarily found in the commercial carbon material) are eliminated. These precursors resulted in the production of submicron and uniform TiC particles with loose agglomeration. Fig. 3 shows the XRD patterns for the TiC formed from the three precursors which were reacted at 1550°C for 4 hours in flowing argon gas. No second phase was detected in these patterns.

Fig. 4a is a TEM micrograph of TiC from the precursor containing (30.95 wt.%-30F) carbon. As seen in Fig. 4a, TiC particles are moderately agglomerated and sintered together because of the limited availability of required amount of carbon. From Equation 2, the theoretical required amount of carbon in the precursor is calculated to be 31.08 wt.%.

$$TiO_2 + 3C = TiC + 2CO \quad (2)$$

The absence of unreacted carbon indicates the carbon has been consumed during the formation of TiC. Particles range in size from 0.1 μm to 0.3 μm.

Fig. 4b is a TEM micrograph of TiC from the precursor containing (32 wt.%-32F) carbon. The particle size and the degree of agglomeration both decreased. The presence of free carbon is noted. The particles shown are uniform with the exception of unreacted carbon. The TiC particles range in size from 0.03 μm to 0.16 μm.

Fig. 4c is a TEM micrograph of TiC from the precursor containing (34 wt.%-34F) carbon. The amount of free carbon increased compared with Fig. 4a and b. The TiC particles are loosely agglomerated with the particles being mostly spherical with ranging in size from 0.02 μm to 0.1 μm.

It was apparent from the TEM micrographs that the degree of agglomeration was decreased with an increase in carbon content in the precursors. Since the TiO_2 particles were totally covered by pyrolytic carbon, the unreacted carbon layer, which exceeded the carbon needed in the reaction, separated the particles after TiC formation. In particular the lower the initial carbon content the level of the agglomeration the more were due to reversed reaction of reduction. Thus agglomeration and particle growth occurred.

The Ti-C phase diagram [6], indicates that TiC, which has the NaCl-type fcc crystal structure, exists over a very wide compositional range. The C/Ti atomic ratio ranges from 0.45 to 0.96. There are few reports about the change of the particle size when the C/Ti ratio changes. According to these reports, the particle size of final product decreases with increased precursor carbon content. The increasing carbon content in the reactants may result in an increase of the C/Ti ratio in TiC_x which may lead to the decrease of the TiC particle size. However, it is not clear that how effective is this mechanism yet.

Oxygen and total carbon content were evaluated to check the purity of the produced TiC powders. Fig. 5 shows these values as a function of initial carbon content in the precursors. The oxygen content decreased when the initial carbon content was increased. The profile of the total carbon content is opposite to that shown in the oxygen content. The lattice parameter of the produced TiC was calculated as a function of initial carbon content and listed in Table I. The lattice parameter of commercial TiC powder (HC starck) was also calculated for comparison and is included in the table. The lattice parameter slightly varied as a function of initial

TABLE I Lattice parameter of TiC as a function of initial carbon content in the precursors

Powder, TiC	Lattice parameter (Angstrom)
30F	4.332
32F	4.333
34F	4.327
HSC	4.331

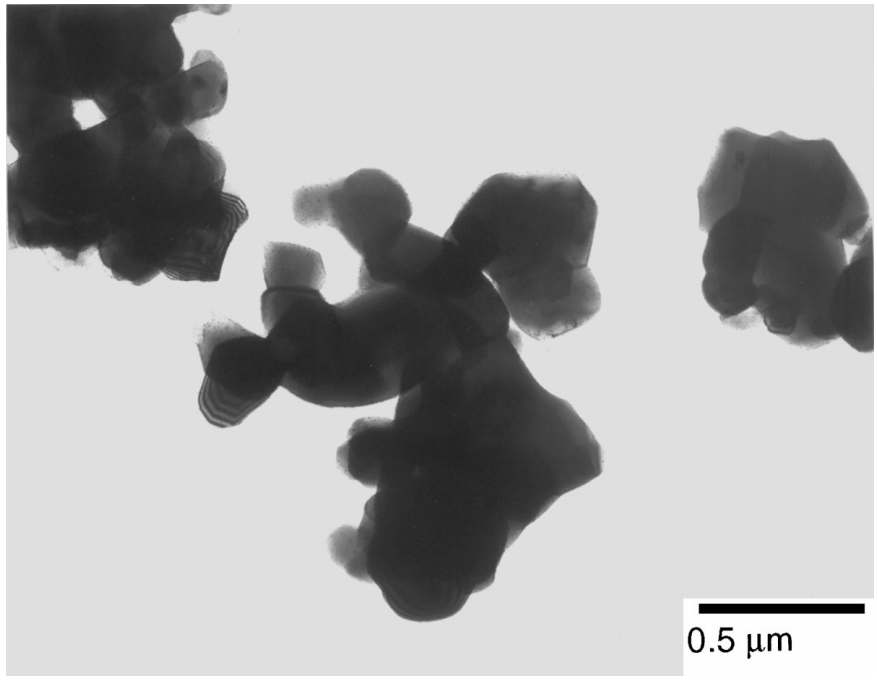

(a)

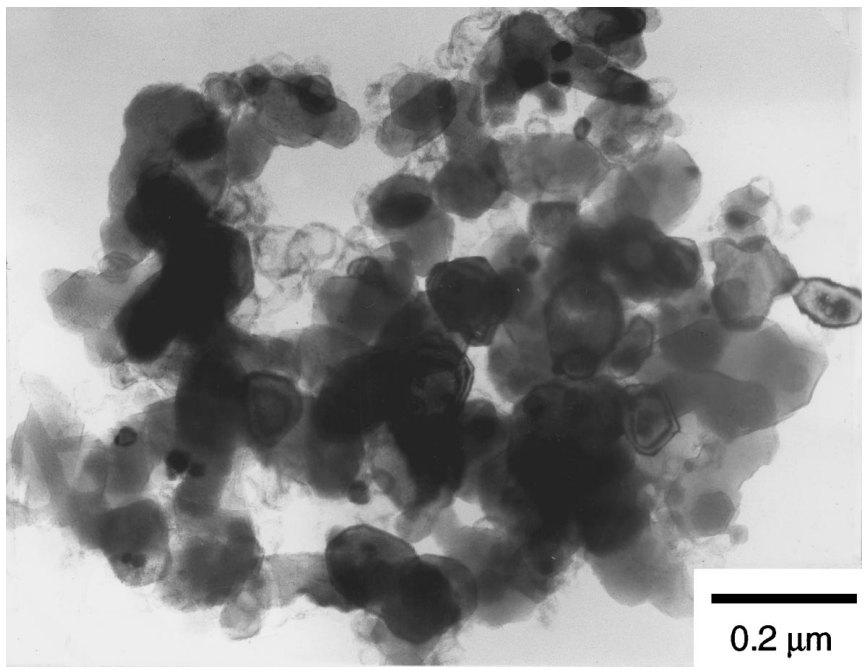

(b)

Figure 4 TEM micrographs of reaction products as a function of carbon content in the precursors. (a) 30F, (b) 32F, (c) 34F. (*Continued*.)

carbon content and they were in an agreement with the lattice parameter of commercial TiC.

Sintering studies were performed in flowing Ar-10%H_2 gas at a temperature of 1500°C using Ni binder. Fig. 6 shows the results of sintered density measurements of TiC-20 wt.% Ni compacts for the various TiC powders. These values correlate with 97%TD for the 30F, 89% TD for the 32F, and 68% TD for the 34F TiC produced powders. Theoretical density of TiC-Ni was calculated to be 5.72 g/cm^3. It was clear that higher sintered density was obtained as the carbon content was decreased. This indicates that the densification rate is faster for TiC powders with lower carbon content. These results are consistent with the previously mentioned work of Exner *et al.* [7] on TiC_x-Ni composites with excess carbon.

The SEM micrographs of sintered and polished surfaces of TiC powders produced with various initial carbon content are shown in Fig. 7. Sintering was performed at 1500°C for 2 hours in flowing Ar-10%H_2. Liquid phase distribution around TiC grains in the high carbon content sample (Fig. 7c) was less uniform than in the sample with low carbon content (Fig. 7a). It is apparent that high porosity exists in the samples with higher total carbon. The TiC (30F) showed the highest sintered densities. This may be due to lack of free carbon and an increase in x value in TiC_x. Free carbon is known to decrease the wettability of TiC by Ni. In addition, the

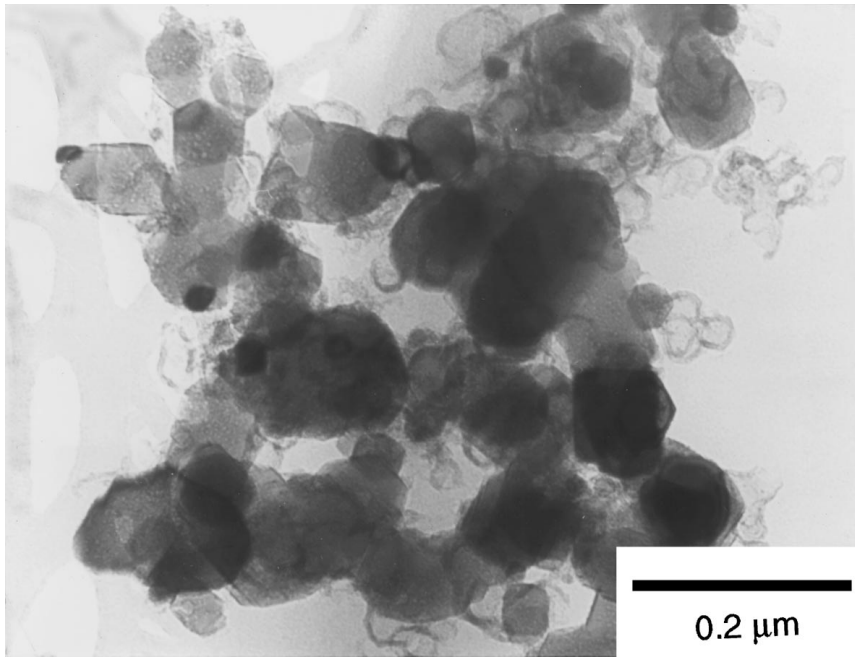

(c)

Figure 4 (*Continued*.)

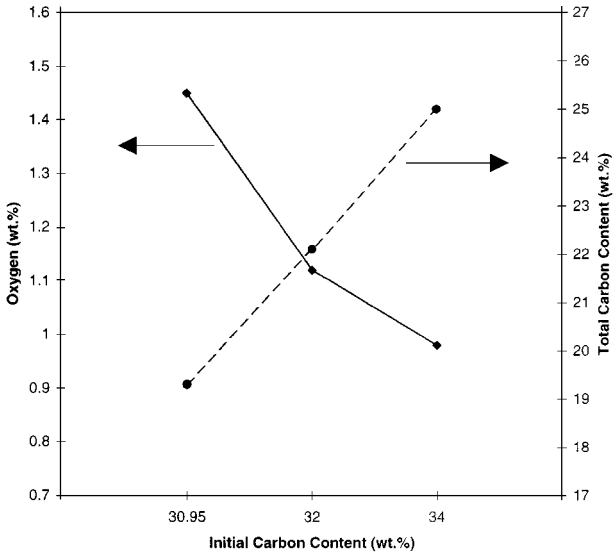

Figure 5 Oxygen and total carbon content as a function of initial carbon content in the precursors.

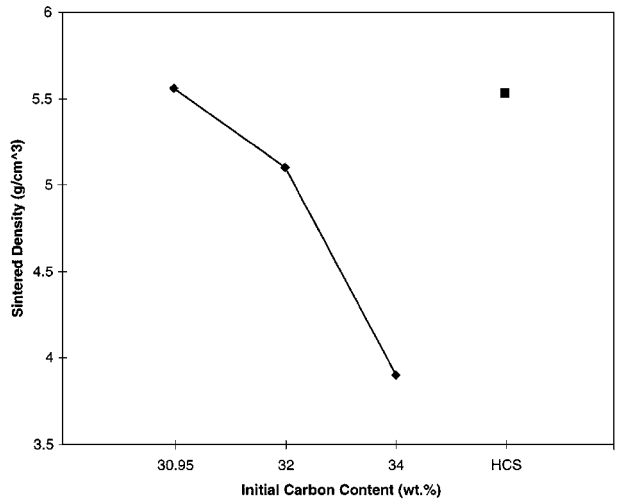

Figure 6 Sintered density as a function of initial carbon content in the precursors.

diffusion coefficient and activation energies for mass transport of C in TiC were found to increase with decreasing free and combined carbon content [8]. It was expected that the diffusion of C in low carbon TiC_x would be much faster than in high carbon TiC_x. The reduced diffusion of carbon within the sample may also have inhibited the sintering [9].

Fig. 8 shows SEM micrograph of commercial TiC (HCS)-20 wt% Ni sample sintered at the same conditions as the produced submicron TiC. A sintered density of 96% TD was achieved after sintering with 20 wt% Ni. The TiC grains were irregularly round and separated by Ni matrix, while in Fig. 7a, the microstructure of TiC (30F)–20 wt.% Ni shows angular TiC grains embedded in a nearly continuous Ni binder. In comparing Figs 7a and 8, the HC Starck TiC grains are coarser and more round than the TiC grains in Fig. 7a. As it can be seen from Fig. 8, the TiC grains are surrounded by a layer which is not found in the TiC (product)-Ni system. EDAX was employed to analysis this third phase. The results indicated that there is Ti content in the binder phase and the surrounding layer consists of (Ti, Ni)C. These were indications of the TiC powders produced from carbon coating method were more stoichiometric than that of commercial TiC.

In order to describe the sintering behavior of TiC (30F) powder and the HC Starck powder with 20 wt.% Ni, DSC was utilized. Pellets of each were broken, to accommodate the size restriction of the Labsys TG-DTA/DSC apparatus (Setaram Corp., Caluire, France). Multiple samples were reacted under flowing argon. Sintering run consisted of heating the samples at 20°C/min to 1500°C, then cooling the samples

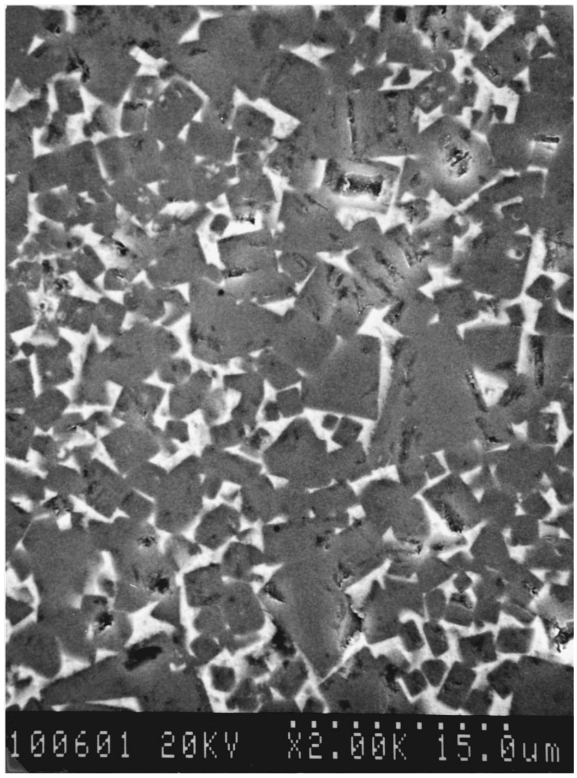

(a)

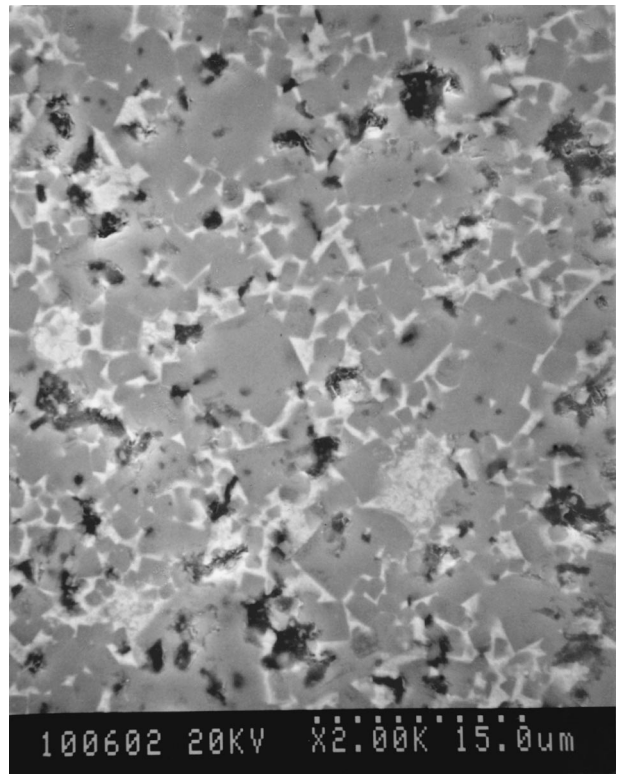

(b)

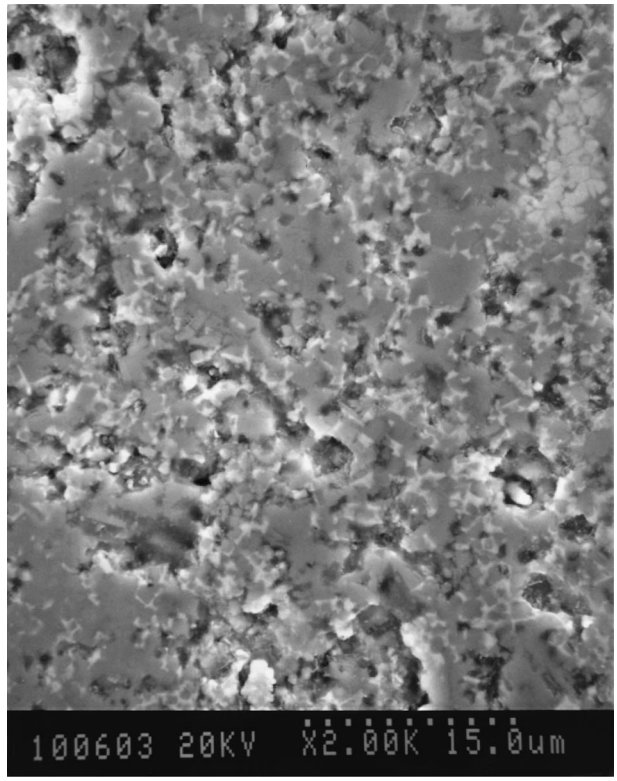

(c)

Figure 7 SEM micrographs of TiC-20 wt.% Ni sintered at 1500°C for 2 hours in flowing Ar+10%H_2. (a) 30F, (b) 32F, (c) 34F.

immediately. The DSC curves are shown in Fig. 9. From the DSC curves it is apparent that commercial TiC (HCS) undergoes a second endothermic reaction, while the product TiC (30F) powder only one. The second reaction proceeds immediately upon completion of the first. This can be explained as the first curve accomplishing the formation of the Ni liquid phase, with the second being the formation of the Ni_xTi_y third phase.

Examination of the Ti-Ni phase diagram [6] yields identification of the third phase. At 1304°C Ni_3Ti intermetallic compound has an eutectic near this

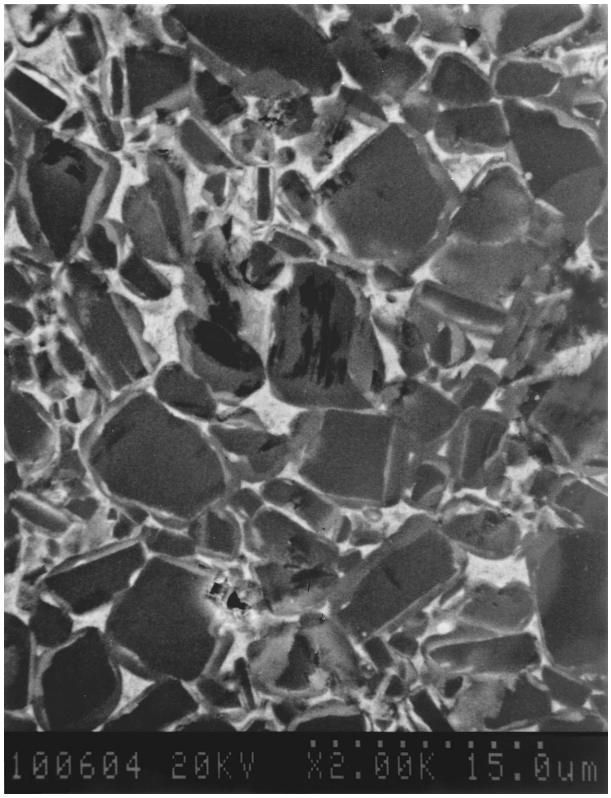

Figure 8 SEM micrograph of TiC(HCS)-20 wt.% Ni sintered at 1500°C for 2 hours in flowing Ar-10%H_2.

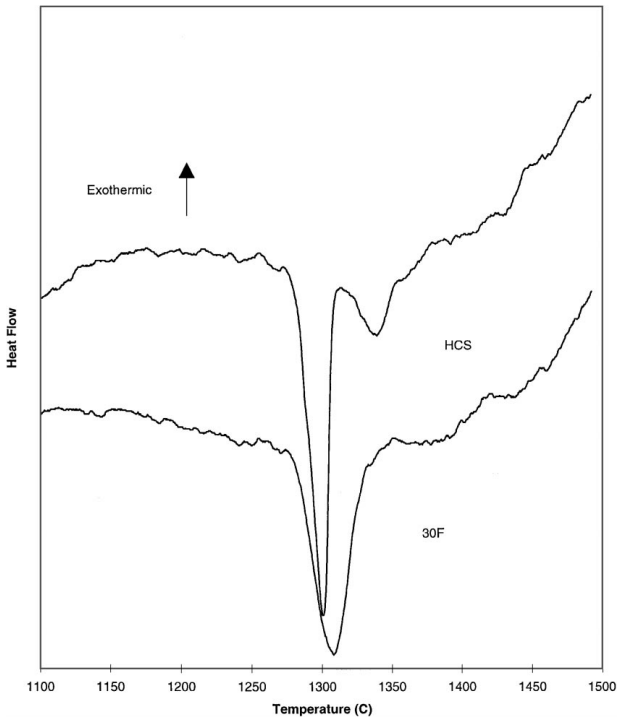

Figure 9 DSC curves of TiC(30F)- and TiC(HCS)-20 wt.% Ni pieces of pelets heated in a Pt crucible at 20°C/min to 1500°C in flowing Ar.

temperature. This temperature corresponds very closely with inception temperature of the second endothermic formation for the commercial powder. This composition, Ni_3Ti, would make sense, as there cannot be a very large amount of free Ti in the commercial powder as compared with the amount of Ni in the compact. The lack of second reaction in the TiC produced

TABLE II Vickers hardness and fracture toughness values as a function of precursor carbon content

Sample	Vickers hardness (kg/mm^2)	Fracture toughness ($MPa{\cdot}m^{1/2}$)
TiC(30F)-20 wt.% Ni	1295	11.09
TiC(32F)-20 wt.% Ni	1024	10.55
TiC(34F)-20 wt.% Ni	219	7.9
TiC(HCS)-20 wt.% Ni	1189	10.99

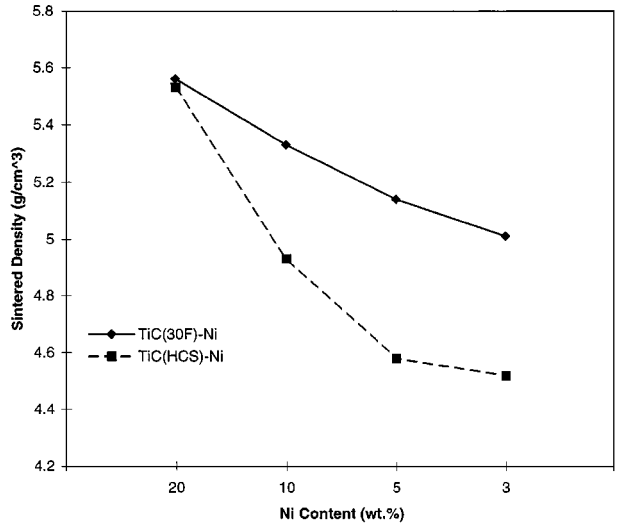

Figure 10 Sintered densities for TiC(30F) and TiC(HCS) as a function of Ni content (Sintering temperature: 1500°C, time: 2 hours, atmosphere: Ar-10%H_2).

from carbon coating method correlates with the higher amount of total carbon and a lack of free Ti. The DSC studies confirmed that the submicron TiC powders are more stoichiometric than the commercially available HC Starck TiC powder.

Hardness measurements of TiC-20 wt% Ni according to initial carbon content is shown in Table II. The TiC-Ni system with the lowest carbon content exhibited the highest hardness. It is not possible to isolate the effect of microstructural changes, due to the presence of porosity, on the mechanical behaviors. This is caused by increased porosity coinciding with increased carbon. In Table II, the fracture toughness values are included as a function of initial carbon content in the precursors. The change in fracture toughness with carbon content followed a general trend similar to that of hardness.

Since TiC-based cermets are mainly used as cutting tools and wear resistant parts which need high hardness, a smaller amount of Ni binder is preferred although the larger Ni additions tend to enhance the fracture toughness of the product [10]. In order to determine the effect of the amount of Ni binder on the densification of TiC (30F) powders—Ni and TiC (HCS)-Ni systems, 3 wt% (TD = 5.05 g/cm^3), 5 wt% (TD = 5.13 g/cm^3), 10 wt% (TD = 5.33 g/cm^3) and 20 wt% (TD = 5.72 g/cm^3) Ni were used. The sintered densities of TiC (30F) and TiC(HCS) with various amounts of Ni, sintered at 1500°C for 2 hours under flowing Ar+10H_2 gas, are shown in Fig. 10. Despite the fact that the Ni content of the samples varied from 3 to 20 wt%, the sintered densities of product TiC (30F)-Ni cermet exhibited a

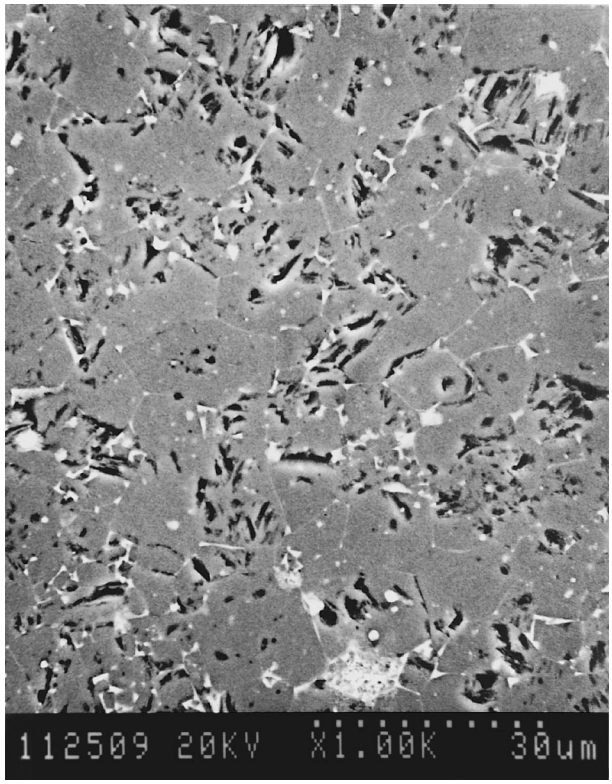

(a)

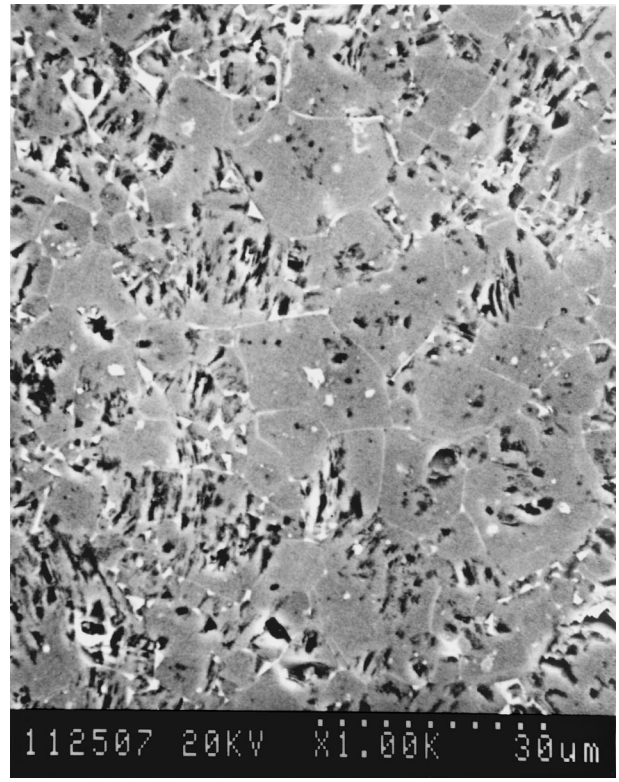

(b)

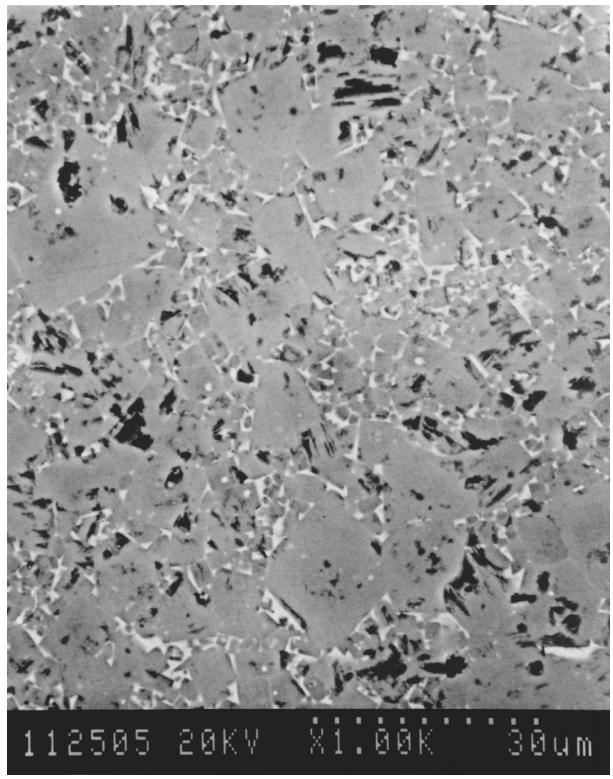

(c)

Figure 11 SEM micrographs of TiC(30F)-Ni wt.% sintered at 1500°C for 2 hours in flowing Ar-10%H_2. (a) 3 wt.% Ni, (b) 5 wt.% Ni, (c) 10 wt.% Ni.

very small range of variance: 99, 100, 99, and 97% TD, for 3, 5, 10, and 20 wt.% Ni, respectively. An important observation of the submicron TiC (30F)-Ni system was that the lowest sintered percent of TD was obtained for the greatest Ni content. However, the sintered densities of TiC(HCS)-Ni system decreased considerably with the decrease of Ni content: 89, 89, 92, and 96% TD for 3, 5, 10, and 20 wt% Ni, respectively.

The SEM micrographs of polished surfaces of these samples are shown in Fig. 11a–c for the submicron TiC (30F)—3, 5, and 10 wt.% Ni, respectively. Clearly, the particles were in contact during sintering and the

contiguity of particles increased with decreasing Ni content. The microstructure consists of TiC grains with a discontinuous Ni layer located at the boundaries and triple points. The Ni is discontinuous because it does not completely wet TiC in the liquid state. Closer examination of the structure indicated that the apparent large carbide grains were not single grain but possessed a mosaic structure typical of polycrystalline aggregates. This type of structure is due to the agglomeration of TiC powders and a mechanism resulting from the incomplete wetting of the carbide particles by Ni. If the liquid Ni phase is unable to penetrate intergranular spaces

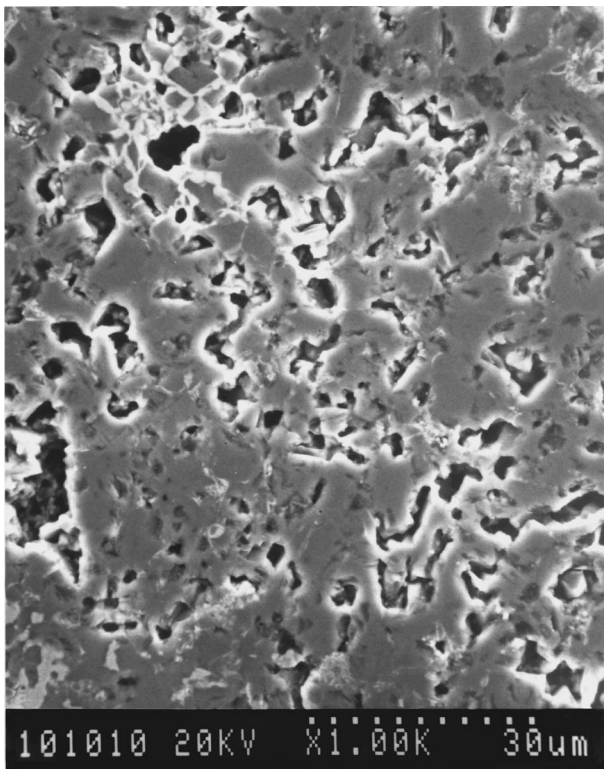

(a)

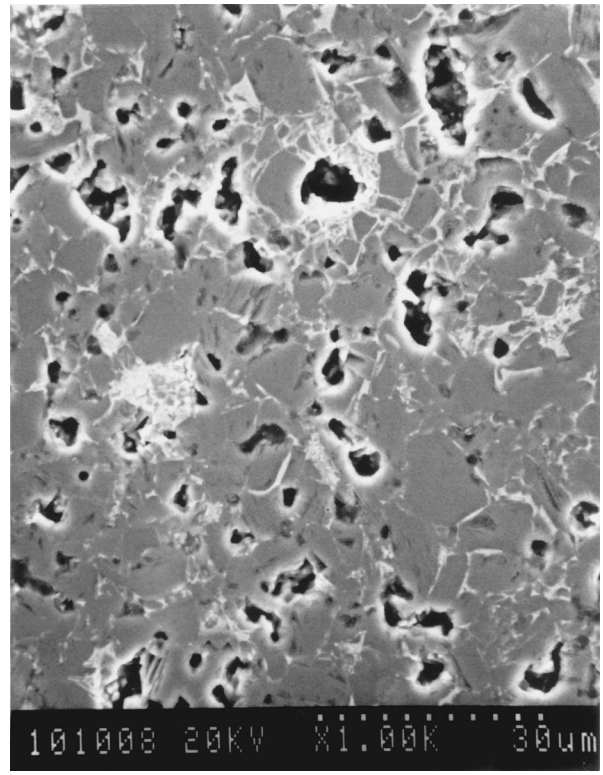

(b)

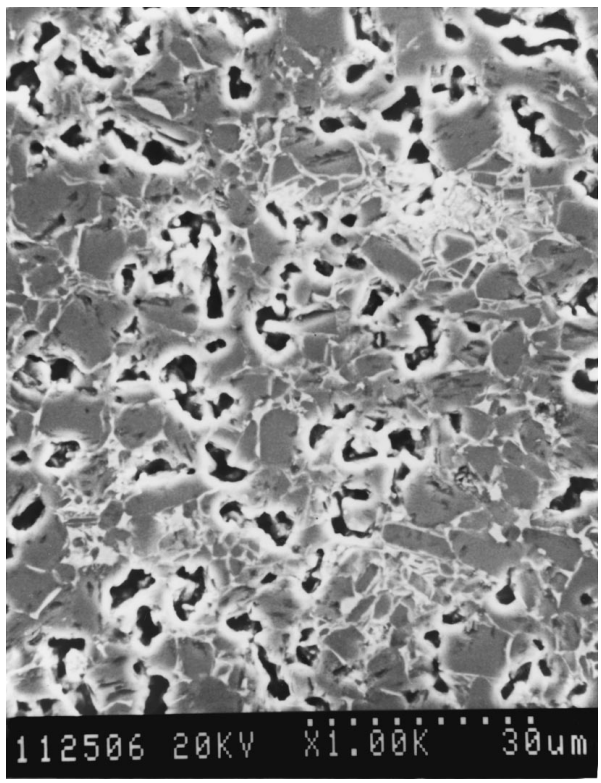

(c)

Figure 12 SEM micrographs of TiC(HCS)-Ni wt.% sintered at 1500°C for 2 hours in flowing Ar-10%H_2. (a) 3 wt.% Ni, (b) 5 wt.% Ni, (c) 10 wt.% Ni.

and completely disperse the solid phase, the particles are drawn together during the consolidation process. The resulting TiC (30F)-Ni exhibits a microstructure of coalesced nonmetallic grains.

Fig. 12a–c show the SEM photomicrographs of TiC(HCS)—3, 5, and 10 wt%, Ni, respectively. With the decrease of Ni content, vermicular microstructure of elongated pores and grains developed. Observation of microstructural developments clearly illustrated the different characteristic behavior of the two materials. At lower Ni content, it was apparent that much lower densification was attained with HC Starck powders. The increased Ni content reduced the energy required for densification [11]. When the Ni content fell below a certain amount, the surface energy (particle size of TiC powders) became the dominant factor influencing the densification. Submicron TiC powders produced from the new process give a higher densification due both to an increase in the capillary forces resulted from high surface area and to a decrease in the distance of matter transport needed to fill pores. So submicron TiC powders achieved almost full densification even with very small amount of Ni binder. Comparatively, the TiC(HCS)-Ni system was found to be more porous because the large particle size resulted in poorer densification.

The Vickers hardness as a function of Ni content is shown in Fig. 13 for the TiC (30F)-Ni and TiC(HCS)-Ni systems. As expected, the hardness of TiC (30F)-Ni cermets showed an increasing trend with decreasing Ni content. This is due to the larger amount of hard phase with less Ni binder. The change of the hardness of TiC(HCS)-Ni displayed an opposite trend to that of the TiC (30F)-Ni cermets produced using submicron TiC powders. This opposite behavior is attributed to increase of porosity in the structure with decrease of the Ni content. It is worth noting that for like amounts of Ni content, the hardness of TiC(HCS)-Ni is lower than that of TiC(30F)-Ni. The relatively low hardness can be explained on the basis of coarser grain size and higher porosity.

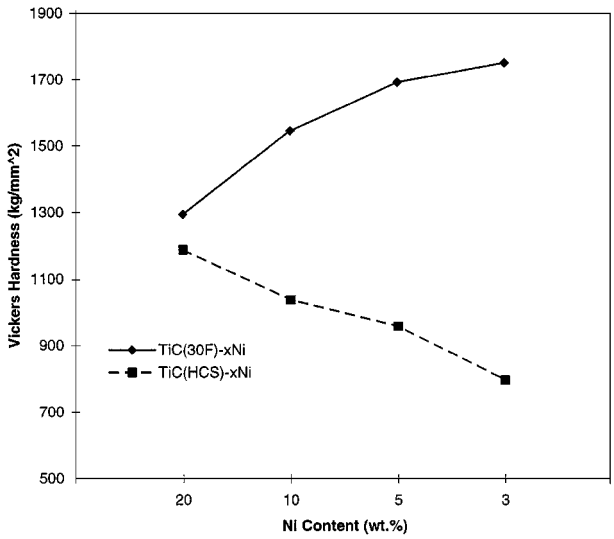

Figure 13 Vickers hardness of TiC(30F) and TiC(HCS) as a function of Ni content.

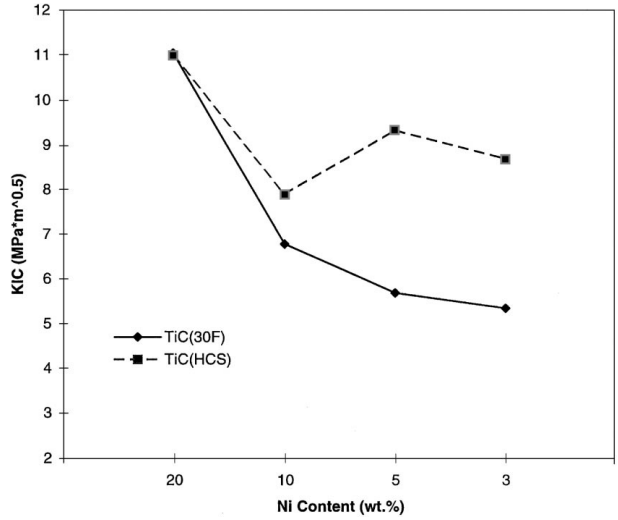

Figure 14 Fracture toughness of TiC(30F) and TiC(HCS) as a function of Ni content.

The initial investigations attempt to provide information on the sinterability of submicron TiC powders produced using a new carbon coating method. It is also intend of this paper to study hardness and fracture toughness of resulting TiC-Ni. There are several experimental techniques by which fracture toughness, K_{IC}, can be measured. The use of the Vickers hardness indentations to determine K_{IC} has become the preferred method due to its simplicity. This method entails measuring the lengths of the cracks emanating from hardness indentations. Since the three-dimensional path of the crack cannot be measured, error is automatically introduced into calculations which rely on crack length measurements. Using the technique developed by Anstis [12], following Equation 3 is employed for the determination of fracture toughness of the sintered TiC-Ni samples.

$$K_{IC} = \xi \left(\frac{E}{H_v} \right)^{1/2} P C_0^{-3/2} \tag{3}$$

where: K_{IC}: Fracture toughness, ξ: Constant value of 0.016 ± 0.004, H_v: Vickers hardness, E: Young's modulus, P: Indentation load, C_0: the average crack length measured from the center of the indent.

Fig. 14 shows the relationship between the fracture toughness and Ni content for the both systems. As expected, the fracture toughness of TiC(HCS)-Ni is higher than that of TiC(30F)-Ni. Because the Vickers hardness indentation method was used to measure the fracture toughness, this parameter depends on the crack length. The presence of porosity inhibited the propagation of cracks and led to high fracture toughness values. Also, the presence of the third, Ni_xTi_y, phase could slightly increase the fracture toughness of fully densified samples of TiC(HCS)-Ni.

4. Conclusion

The submicron TiC was synthesized using carbon coated TiO_2 precursors. The XRD patterns showed that the products were single phase TiC. The total carbon content in TiC increased with increased initial carbon

content. The produced powders with higher carbon content have finer particle size, looser agglomeration and lower oxygen content.

With 30.95 wtpowders showed:

– fine particle size (0.1–0.3 μm)
– oxygen content of 1.45 wt%
– total carbon content of 19.3 wt%
– lattice parameter of 4.332 Angstrom
– moderate agglomeration

With 32 wt% initial carbon content in the precursor, the resultant TiC (32) powders showed:

– fine particle size (0.03–0.2 μm)
– oxygen content of 1.12 wt%
– total carbon content of 22.1 wt%
– lattice parameter of 4.333 Angstrom
– loose agglomeration

With 34 wt% initial carbon content in the precursor, the resultant TiC (34F) powders showed:

– fine particle size (0.02–0.1 μm)
– oxygen content of 0.98 wt%
– total carbon content of 25 wt%
– lattice parameter of 4.327 Angstrom
– loose agglomeration

TiC-20 wt.% Ni cermets were made through liquid phase sintering, at 1500°C for 2 hours in flowing Ar-10%H_2 gas. As the carbon content increased, the sintered density decreased. The reduction of densification was explained on the basis of the composition variation and the wettability change due to excess carbon. As a result, the Vickers hardness and fracture toughness also decreased with increased carbon content. From the SEM micrographic observations, the morphologies of HC Starck commercial TiC grains were more round and they were surrounded by a third phase. Energy dispersive X-ray (EDX) analysis and DSC results indicated that it is composed of Ni_xTi_y intermetallic, possible Ni_3Ti.

Sintered density of 99 %TD was obtained for sintered submicron TiC (30F) powders with Ni as low as 3 wt.%, at 1500°C for 2 hours in flowing Ar-10%H_2 gas. With decreased Ni content, the Vickers hardness increased and the fracture toughness decreased, as expected. However, the high densification cannot be achieved for commercial HC Starck TiC sintered with Ni ($<$10 wt%) under the same conditions. Both the Vickers hardness and fracture toughness decreased as the Ni content decreased, due to the increase of porosity in the sintered sample.

Acknowledgements

The authors would like to thank Dr. Charles Sorrell for his continuing interest in this work. This research was sponsored by the U.S. Department of Energy, Office of Industrial Technologies, as part of the Advanced Industrial Materials Program, under contract DE-AC05-84OR21400 with Lockheed Martin Energy Systems, Inc.

References

1. I. J. McCOLM and N. J. CLARK, *High Performance Ceramics* (Blackie, London 1986), pp. 60–107.
2. R. KOC and J. S. FOLMER, *J. of Materials Science* **32** (1997) 3101.
3. W. D. KINGERY, *J. of Applied Physics* **30** (1959) 3.
4. R. M. GERMAN, "Liquid Phase Sintering" (Plenum Press, New York, 1985).
5. R. KOC and G. GLATZMAIER, U.S. Patent No: 5,417,952 (1995).
6. T. B. MASSALSKI, "Binary Alloy Phase Diagrams," 2nd ed. (ASTM Int., Materials Park, OH, 1990).
7. H. E. EXNER, E. S. MARTA and G. PETZOW, "Modern Developments in Powder Metallurgy" (Plenum Press, New York, 1971).
8. S. SARIAN, *J. Appl. Phys.* **39** (1968) 3305.
9. M. A. JANEY, *Am. Ceram. Soc. Bull.* **65**(2) (1986) 357.
10. K. J. A. BROOKES, "World Directory and Handbook of Hard-Metals," 2nd ed. (Engineers' Digest, London, 1979).
11. J. C. LASALVIA, M. A. MEYERS and D. K. KIM, *J. of Mater. Synthesis and Processing* **2** (1994) 4.
12. G. R. ANSTIS, *J. Am. Ceram. Sco.* **64**(9) (1994) 533.

Received 26 October 1998
and accepted 19 November 1999